Journal of Applied Electrochemistry **33**: 725–732, 2003.

Multiple-step constant current density electrodeposition of continuous metal material with high porosity

D.L. WANG[1,*], C.S. DAI[1], N. WU[1], Z.H. JIANG[1] and J. LI[2]
[1]*Department of Applied Chemistry, Harbin Institute of Technology, P.O. Box 411, Harbin, 150001, China*
[2]*School of Chemical Engineering, Georgia Institute of Technology, Atlanta, GA 30332-0100, USA*
*(*author for correspondence, e-mail: nwu@public.hr.hl.cn)*

Received 28 September 2002; accepted in revised form 22 April 2003

Key words: constant current density, continuous porous metal material, multiple-step electrodeposition

Abstract

A mathematical model has been established to analyse the cathode current during the production of continuous porous metal using a multiple-step electrodeposition technique. The electrodeposition parameters and production line have been optimized to maintain constant current density on the cathode during the process. The continuous nickel foam thus produced has an improved microstructure and mechanical properties.

List of symbols

A	surface density of porous metal after multi-step electrodeposition (kg m^{-2})
$D_i(x)$	distance between anode and cathode at point x in the ith plating region (m)
F	faradaic constant (C mol^{-1})
H	width of the porous metal cathode (m)
$I_i(x)$	cathodic current flowing through cathode at point x in the ith plating region (A)
I_i	cathodic current in the ith plating region (A)
j	constant cathodic current density for multistep electrodeposition (A m^{-2})
K	constant for the superficial resistivity of the continuous porous metal (kg m^{-3})
L_i	length of the ith plating region (m)
l_i	distance between the baffle in the ith plating region and the conductive roll close to the baffle (m)
M	molecular weight of the metal (g mol^{-1})
M_i	mass of metal deposited per unit cathode volume in the ith plating region (kg m^{-3})
$M_i(x)$	mass of metal deposited per unit cathode volume reaching point x in the ith plating region (kg m^{-3})
n'	number of electrons transferred in metal reduction
$Q_i(x)$	charge passing through per unit length cathode before reaching a point x in the ith plating region during process (C m^{-1})
$R_i(x)$	superficial resistance of continuous porous metal at point x in the ith plating region (Ω)
υ	velocity of porous metal cathode during process (m s^{-1})
S	cross-sectional area of porous metal cathode (m^2)
$U_i(x)$	potential difference between anode and cathode at point x in the ith plating region (V)
$U_{ri}(x)$	total cathode and anode overpotential at point x in the ith plating region (V)
U	potential difference between anode and conductive roll (V)
η	cathodic current efficiency
ρ_0	true metal resistivity (Ω m)
ρ_L	electrolyte resistivity (Ω m)

1. Introduction

Porous metal materials are playing an important role as functional structural materials due to their large specific surface area and good conductivity. They are widely used as catalyst carriers, filters, electromagnetic screens, and electrode current collectors in rechargeable batteries, fuel cells, capacitors, and in electrochemical synthesis [1–6]. Electrodeposition is one of the most important techniques used to produce porous metal materials: a

metal or alloy is electrochemically deposited on the previously metallized porous polyester sponge substrate, and then the polyester is removed through pyrolysis in hydrogen or an inert atmosphere. The porous metal thus produced is of uniform three-dimensional net-like structure and the porosity is normally above 95%.

Since the superficial resistivity of porous metal is higher than that of the solid metal and depends on its density, the resistivity of the porous metal varies with the deposition time and affects the cathodic current density during electrodeposition. This affects the microstructure and properties of the porous metal [7–10]. Therefore, it is very important to control the constant cathodic current densities during the electrodeposition of porous metal. Langlois et al. investigated the potential and current density distribution in the thickness direction of porous metal when the cathode is motionless [11, 12]. However, the cathode moves with respect to the anode during the electrodeposition of continuous porous metal. The cathodic current distribution is also associated with the velocity of the cathode and its location in relation to the anode. In this paper, a mathematical model is presented to analyse the current distribution in the moving porous metal cathode, and the multistep electrodeposition is optimized to maintain constant cathodic current density. The theoretical analysis has been used to assist in the production of continuous nickel foam.

2. Multistep electrodeposition of continuous porous metal

Figure 1 shows the scheme for multistep constant current density electrodeposition of continuous porous metal. The conductive polyester sponge as the substrate (cathode) enters the electrolyte on the left-hand side of the plating tank, horizontally passes N successive plating regions (N is odd), and comes out of the electrolyte with the deposited metal on the right-hand side of the plating tank. There is a pair of conductive rolls and baffles between the nth and the next (the mth) plating regions ($n = 1, 3, 5 \ldots N$; $m = 2, 4, 6 \ldots N - 1$). The baffles separate the anode in the nth plating region from the anode in the mth plating region. Thus, the function of the baffles is to prevent possible metal deposition on the conductive rolls. The conductive rolls support the cathode during transportation and also serve as the electrical connection to the cathode. The anodes lie symmetrically at the opposite sides of the cathode.

The detailed configuration of the nth and mth plating regions ($n = 1, 3, 5 \ldots N$; $m = 2, 4, 6 \ldots N - 1$) is shown in Figure 2. The cathode moves in the electrolyte in the direction perpendicular to the baffles. In the nth plating region, the length of the plating region is L_n and covers the distance between the baffle at the right-hand side and the point at the left-hand side where the distance between the cathode and the anode is the shortest. $x = 0$ is set at the location of the baffle because the cathodic current flows through the cathode from the conductive roll and in the opposite direction to the cathode movement. The distance between the cathode and the anode is $D_n(x)$ and depends on the cathode location in the plating region. The distance between the baffle and the conductive roll is l_n. In the mth plating region, the length of the plating region is L_m and covers the distance between the baffle at the left-hand side and

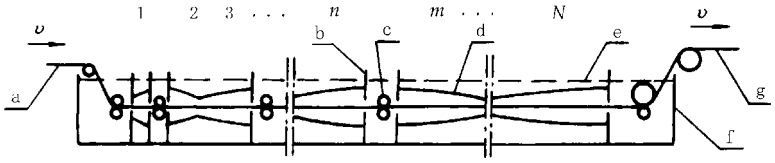

Fig. 1. Scheme for multistep constant current density electrodeposition of continuous porous metal with N successive plating regions (1, 2, 3, ... ,n, m ..., $N - 1$, N). Key: (a) conductive polyester sponge; (b) baffle; (c) conductive roll; (d) anode; (e) electrolyte; (f) plating tank; (g) conductive polyester sponge with the deposited metal.

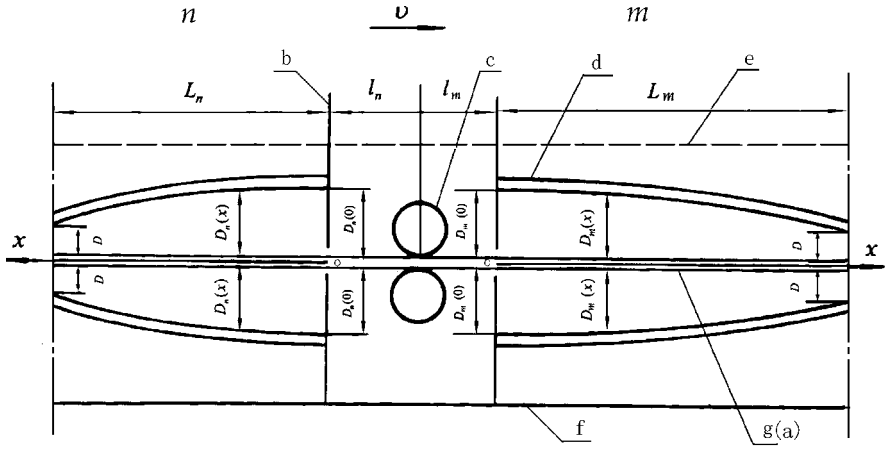

Fig. 2. Detailed configuration of the nth and mth successive plating regions. Key: (a) or (g) conductive polyester sponge with the deposited metal; (b) baffle; (c) conductive roll; (d) anode; (e) electrolyte; (f) plating tank.

the point at the right-hand side where the distance between the cathode and the anode is the shortest. $x = 0$ is set at the location of the baffle because the cathodic current flows through the cathode from the conductive roll and in the same direction as the cathode moves. The distance between the cathode and the anode in the plating region is $D_m(x)$; the distance between the baffle and the conductive roll is l_m. To eliminate current density edge effects, the width of the cathode and anode in each plating region are exactly the same. Further, the distance between the cathode and anode at one side of a plating region is equal to the corresponding side of the next plating region and is a constant, that is

$$D_i(0) = D(0) \qquad i = 1, 2, 3, \ldots N-1, N \tag{1}$$

$$D_i(L_i) = D \qquad i = 1, 2, 3, \ldots N-1, N \tag{2}$$

3. Mathematical model

Based on multistep constant current density electrodeposition and the characteristics of continuous porous metal, three fundamental postulates are proposed for the building of the mathematical model:

I. The superficial resistivity of a porous metal is proportional to the true resistivity of the metal and has the same characteristics as that of the solid metal. That is, the superficial resistivity of the porous metal is inversely proportional to the metal density and its cross-sectional area.

II. The cathodic current efficiency of the metal electrodeposition is constant. The width and the thickness of the cathode are constant during the process.

III. The cathode moves at constant velocity in the electrolyte during the process. The change in the mass, structure, and properties of the porous metal during deposition with time is only determined by the cathode location in a plating region. The porosity of the cathode is constant during the process.

Since the cathode thickness is tiny compared with its width and length, the cathodic current through the cathode cross-section area may be neglected. The cathodic current through unit length of cathode in a plating region is

$$I_i = 2jHL_i \quad i = 1, 2, 3, \ldots N-1, N \tag{3}$$

Thus, when the cathode reaches point x after entering the nth plating region, the charge passing through unit length of cathode can be expressed as

$$Q_n(x) = \frac{2Hj}{\upsilon}(L_n - x) \quad n = 1, 3, 5, \ldots N \tag{4a}$$

When the cathode reaches point x in the mth plating region, the charge through unit length of cathode is

$$Q_m(x) = \frac{2Hj}{\upsilon}x \quad m = 2, 4, 6, \ldots N-1 \tag{4b}$$

Thus, the mass of deposited metal per unit cathode volume when the cathode reaches point x in the nth plating region is

$$M_n(x) = \frac{2 \times 10^{-3} M\eta jH}{n'FS\upsilon}(L_n - x) \quad n = 1, 3, 5, \ldots N \tag{5a}$$

The mass of deposited metal per unit cathode volume before reaching point x in the mth plating region is

$$M_m(x) = \frac{2 \times 10^{-3} M\eta jH}{n'FS\upsilon}x \quad m = 2, 4, 6, \ldots N-1 \tag{5b}$$

In the same way, the total mass of deposited metal per unit cathode volume in a plating region is

$$M_i = \frac{2 \times 10^{-3} M\eta jHL_i}{n'FS\upsilon} \quad i = 1, 2, 3, \ldots N-1, N \tag{6}$$

From hypothesis, the superficial resistance of the porous metal cathode with length dx at point x in the nth plating region is defined by Equation 7(a)

$$\mathrm{d}R_n(x) = \frac{K\rho_0}{S\left[\sum_{i=1}^{n-1} M_i + M_n(x)\right]}\mathrm{d}x \quad n = 1, 3, 5, \ldots N \tag{7a}$$

where K is the constant for the superficial resistivity of the continuous porous metal and is associated with the structure and deposition process. The superficial resistance of the porous metal cathode with length dx at point x in the mth plating region is defined by Equation 7(b)

$$\mathrm{d}R_m(x) = \frac{K\rho_0}{S\left[\sum_{i=1}^{m-1} M_i + M_m(x)\right]}\mathrm{d}x \quad m = 2, 4, 6, \ldots N-1 \tag{7b}$$

The currents flowing through the cathode at point x in the nth plating region and the mth plating region are given by Equation 8(a) and (b), respectively

$$I_n(x) = 2Hj(L_n - x) \qquad n = 1, 3, 5, \ldots N \tag{8a}$$

$$I_m(x) = 2Hj(L_m - x) \qquad m = 2, 4, 6, \ldots N-1 \tag{8b}$$

Using Ohm's law, the potential drops over cathode length dx at point x in the nth plating region and the m th plating region are, respectively,

$$\mathrm{d}U_n(x) = -I_n(x)\mathrm{d}R_n(x) \qquad n = 1, 3, 5, \ldots N \tag{9a}$$

$$dU_m(x) = -I_m(x)dR_m(x) \quad m = 2, 4, 6, \ldots N-1 \quad (9b)$$

Substituting Equations 6, 7(a), 8(a) and 7(b), 8(b) into Equation 9(a) and (b), respectively, produces Equation 10(a) and (b):

$$dU_n(x) = -\frac{10^3 Kn' F \rho_0 \upsilon (L_n - x)}{M\eta\left[\sum_{i=1}^{n} L_i - x\right]}dx \quad n = 1, 3, 5, \ldots N \quad (10a)$$

$$dU_m(x) = -\frac{10^3 Kn' F \rho_0 \upsilon (L_m - x)}{M\eta\left[\sum_{i=1}^{m-1} L_i + x\right]}dx \quad m = 2, 4, 6, \ldots N-1 \quad (10b)$$

The boundary conditions for Equation 10(a) and (b) are $U_n(x) = U_n(0)$ at point $x = 0$ in the nth plating region and $U_m(x) = U_m(0)$ at point $x = 0$ in the mth plating region, respectively. $U_n(0)$ and $U_m(0)$ are the potential differences between the anode and the cathode at the baffle close to the conductive roll ($x = 0$) in the nth plating region and the mth plating region, respectively. The potential differences between the anode and cathode at point x in the nth plating region and the mth plating region can thus be derived by integration of Equation 10(a) and (b), respectively

$$U_n(x) = U_n(0) - \frac{10^3 Kn' F \rho_0 \upsilon}{M\eta} \times \left[x + \left(\sum_{i=1}^{n-1} L_i\right) \ln\left(1 - \frac{x}{\sum_{i=1}^{n} L_i}\right)\right] \quad n = 1, 3, 5, \ldots N \quad (11a)$$

$$U_m(x) = U_m(0) - \frac{10^3 Kn' F \rho_0 \upsilon}{M\eta} \times \left[-x + \left(\sum_{i=1}^{m} L_i\right) \ln\left(1 + \frac{x}{\sum_{i=1}^{m-1} L_i}\right)\right] \quad m = 2, 4, 6, \ldots N-1 \quad (11b)$$

Since the cathode thickness can be neglected, the potential difference between the anode and the cathode at point x in a plating region can also be expressed by the potential drop through the electrolyte and electrode overpotential

$$U_n(x) = j\rho_L D_n(x) + U_{rn}(x) \quad n = 1, 3, 5, \ldots N \quad (12a)$$

$$U_m(x) = j\rho_L D_m(x) + U_{rm}(x) \quad m = 2, 4, 6, \ldots N-1 \quad (12b)$$

$U_{rn}(x)$ and $U_{rm}(x)$ are the sums of the cathode and anode overpotentials at point x in the nth plating region and the mth plating region, respectively, and both are assumed to be constants due to the constant current density electrodeposition and the same electrolyte temperature and convection in the plating tank. Substituting Equation 12(a) and (b) into Equation 11(a) and (b), respectively, the distance between the cathode and the anode at point x in the nth plating region or the mth plating region is given by

$$D_n(x) = D_n(0) - \frac{10^3 Kn' F \rho_0 \upsilon}{M\eta\rho_L j} \times \left[x + \left(\sum_{i=1}^{n-1} L_i\right) \ln\left(1 - \frac{x}{\sum_{i=1}^{n} L_i}\right)\right] \quad n = 1, 3, 5, \ldots N \quad (13a)$$

$$D_m(x) = D_m(0) - \frac{10^3 Kn' F \rho_0 \upsilon}{M\eta\rho_L j} \times \left[-x + \left(\sum_{i=1}^{m} L_i\right) \ln\left(1 + \frac{x}{\sum_{i=1}^{m-1} L_i}\right)\right] \quad m = 2, 4, 6, \ldots N-1 \quad (13b)$$

In multistep constant current density electrodeposition of continuous porous metal, the cathode velocity can be determined by

$$\upsilon = \frac{2 \times 10^{-3} M\eta j}{n' FA} \sum_{i=1}^{N} L_i \quad i = 1, 2, 3, \ldots N-1, N \quad (14)$$

Substituting Equation 14 into Equation 13(a) and (b) gives

$$D_n(x) = D_n(0) - \frac{2K\rho_0}{A\rho_L}\left(\sum_{i=1}^{N} L_i\right) \times \left[x + \left(\sum_{i=1}^{n-1} L_i\right) \ln\left(1 - \frac{x}{\sum_{i=1}^{n} L_i}\right)\right] \quad n = 1, 3, 5, \ldots N \quad (15a)$$

$$D_m(x) = D_m(0) - \frac{2K\rho_0}{A\rho_L}\left(\sum_{i=1}^{N} L_i\right) \times \left[-x + \left(\sum_{i=1}^{m} L_i\right) \ln\left(1 + \frac{x}{\sum_{i=1}^{m-1} L_i}\right)\right] \quad m = 2, 4, 6, \ldots N-1 \quad (15b)$$

When $n = 1$, Equation 15(a) is

$$D_1(x) = D_1(0) - \frac{2K\rho_0}{A\rho_L}\left(\sum_{i=1}^{N} L_i\right)x \quad (16)$$

Assuming $L_i = a_i L_1$ and $a_1 = 1$, where $x = L_i$, substituting Equations 1 and 2, Equations 16, 15(a) and (b) can be expressed as Equation 17(a), (b) and (c), respectively:

$$\frac{2K\rho_0 L_1^2}{A\rho_L[D(0)-D]}\left(\sum_{i=1}^{N} a_i\right) = 1 \tag{17a}$$

$$\frac{2K\rho_0 L_1^2}{A\rho_L[D(0)-D]}\left(\sum_{i=1}^{N} a_i\right) \times \left[a_n + \left(\sum_{i=1}^{n-1} a_i\right)\ln\left(1-\frac{a_n}{\sum_{i=1}^{n} a_i}\right)\right] = 1 \quad n=3,5,7,\ldots N \tag{17b}$$

$$\frac{2K\rho_0 L_1^2}{A\rho_L[D(0)-D]}\left(\sum_{i=1}^{N} a_i\right) \times \left[-a_m + \left(\sum_{i=1}^{m} a_i\right)\ln\left(1+\frac{a_m}{\sum_{i=1}^{m-1} a_i}\right)\right] = 1 \quad m = 2,4,6,\ldots N-1 \tag{17c}$$

The solutions for Equation 17(a), (b), and (c) are

$$L_1 = \left[\frac{A\rho_L[D(0)-D]}{2K\rho_0 \sum_{i=1}^{N} a_i}\right]^{1/2} \tag{18}$$

$$L_i = a_i L_1 \quad i = 1,2,3,\ldots N-1, N \tag{19}$$

$$a_1 = 1 \tag{20}$$

$$a_2 = e - 1 \tag{21}$$

$$\vdots$$

$$a_n = 1 + \left(\sum_{i=1}^{n-1} a_i\right)\ln\left(1+\frac{a_n}{\sum_{i=1}^{n-1} a_i}\right) \quad n = 3,5,7,\ldots N \tag{22a}$$

$$a_m = -1 + \left(\sum_{i=1}^{m} a_i\right)\ln\left(1+\frac{a_m}{\sum_{i=1}^{m-1} a_i}\right) \quad m = 2,4,6,\ldots N-1 \tag{22b}$$

In multistep constant current density electrodeposition, the length of the anode in each plating region or the length of each plating region is determined by Equations 18, 19, 20, 21, 22(a), and (b). The distance between the cathode and the anode in each plating region is determined by Equations 15(a), (b), and 16.

The cathodic currents in the nth plating region and the mth plating region are obtained from the Equation 8(a) and (b), respectively:

$$I_n = 2jHL_1 a_n \quad n = 1,3,5,\ldots N \tag{23a}$$

$$I_m = 2jHL_1 a_m \quad m = 2,4,6,\ldots N-1 \tag{23b}$$

Thus, the total cathodic current in multistep electrodeposition is

$$I = 2jHL_1 \sum_{i=1}^{N} a_i \quad i = 1,2,3,\ldots N-1, N \tag{24}$$

The potential differences between the cathode and the anode at $x = 0$ in the nth plating region and the mth plating region are given by Equation 25(a) and (b), respectively:

$$U_n(0) = U - \frac{I_n K\rho_0 l_n}{S\sum_{i=1}^{n} M_i} \quad n = 1,3,5,\ldots N \tag{25a}$$

$$U_m(0) = U - \frac{I_m K\rho_0 l_m}{S\sum_{i=1}^{m-1} M_i} \quad m = 2,4,6,\ldots N-1 \tag{25b}$$

where U is the potential difference between the anode and the conductive roll, which is determined by the d.c. power supply. The second terms on the left-hand side of Equation 25(a) and (b) represent the potential drops over the porous metal length between the conductive roll and baffles ($x = 0$) in the nth plating region and the mth plating region, respectively.

Since the cathodic current density is constant during multistep electrodeposition, the cathode and anode overpotential is constant. From Equations 1, 12(a) and (b), the potential difference between the cathode and the anode at $x = 0$ in a plating region is constant. Consequently,

$$U_i(0) = U_n(0) = U_m(0) = U_1(0) \tag{26}$$

Substituting Equation 25(a) and (b) into Equation 26 gives

$$\frac{I_n l_n}{\sum_{i=1}^{n} M_i} = \frac{I_m l_m}{\sum_{i=1}^{m-1} M_i} = \frac{I_1 l_1}{M_1} \tag{27}$$

Substituting Equation 23(a) and (b) into Equation 27 gives

$$l_n = \frac{\sum_{i=1}^{n} a_i}{a_n} \times l_1 \quad n = 1,3,5,\ldots N \tag{28a}$$

$$l_m = \frac{\sum_{i=1}^{m-1} a_i}{a_m} \times l_1 \quad m = 2,4,6,\ldots N-1 \tag{28b}$$

Thus, Equation 28(a) and (b) can be used to determine the distance between the baffle and the conductive roll in a plating region.

4. Experimental details

Five-step electrodeposition was conducted for the fabrication of continuous nickel foam. The electrodeposition nickel electrolyte contained 280 kg m^{-3} nickel sulfate, 35 kg m^{-3} nickel chloride and 40 kg m^{-3} boric acid. Deionized water was used to prepare the electrolyte. The pH was adjusted using NaOH or H_2SO_4 to 4.1. The temperature was held at 55 °C. INOC MF-50LE conductive polyester sponge (made in Japan, the porosity is 100 per inch) was used as the substrate; the width was 0.65 m and thickness 1.60×10^{-3} m.

In the five-step constant current density electrodeposition of continuous nickel foam, the distance between the baffle and the conductive roll in the first plating region was set to $l_1 = 0.100$. The distance between the anode and the cathode at the location of the baffle in each plating region was set to $D(0) = 0.1$ m and the shortest distance between the anode and the cathode in each plating region was set to $D = 0.02$ m.

The average cathodic current efficiency was calculated using Faraday's law. The superficial resistivity of the nickel foam can be defined as

$$K\rho_0 = \frac{aAR}{b} \tag{29}$$

where a and b are the length and width of the specimen for superficial resistance measurement, respectively, R is the superficial resistance of the nickel foam. The superficial resistance for the nickel foam was measured using the double electrical bridge method at 20 °C, and the size of the specimen was 0.20 m in length and 0.01 m in width. The surface density A of the nickel foam was set to 0.5 kg m^{-2} and the actual surface density of the nickel foam produced was examined by changes in the mass of the cathode after five-step electrodeposition. The resistivity of the electrolyte was measured using a DDS-11C conductivity meter.

The microstructure of the nickel foam was observed by means of scanning electron microscopy (SEM). The ultimate tensile strength and elongation of the nickel foam were measured using an Instron-5569 materials tester. The size of specimens was 0.10 m in length, 0.03 m in width, and 1.60×10^{-3} m in thickness. All measurements were carried out at an extension rate of 3.33×10^{-3} m s^{-1}.

5. Results and discussion

The superficial resistivity $K\rho_0$ of continuous nickel foam in each plating region during the five-step electrodeposition is listed in Table 1. The superficial resistivity of the nickel foam thus produced is 3.02×10^{-3} Ω kg m^{-2}.

The resistivity of the electrolyte for the five-step constant current density electrodeposition was 0.214 Ω. Since the surface density A of the nickel foam produced is 0.5 kg m^{-2}, all parameters for the layout of each plating region are given by the above Equations and are listed in Table 2.

The plating line for the five-step electrodeposition was designed according to these parameters. The average cathodic current efficiency for the nickel deposition on the INOC MF-50LE conductive polyester sponge was 95.1%. The optimum constant superficial cathodic current density was 8×10^2 A m^{-2}. The velocity of the cathode in the process was 3.32×10^{-3} m s^{-1}. The total cathodic current for five plating regions was 1864 A.

The microstructure of the nickel foam produced in the non-constant current density electrodeposition is shown in Figure 3 and the microstructure of the nickel foam produced in the designed five-step constant current density electrodeposition is shown in Figure 4. It can be seen that the net structure of both the nickel foams is uniform. The deposited nickel surface using the five-step constant current density electrodeposition is smoother than that using the non-constant current density process. The nickel foam thus produced can maintain the high porosity of the original conductive polyester sponge.

Table 1. Superficial resistivity of nickel foam during the five-step constant current density electrodeposition

Plating region	1	2	3	4	5
A/kg m^{-2}	0.385	0.422	0.453	0.505	0.549
R/Ω	0.159	0.144	0.134	0.119	0.110
$K\rho_0 \times 10^{-3}$/Ω kg m^{-2}	3.06	3.04	3.03	3.00	3.02

Table 2. Parameters for the layout of each plating region in the five-step constant current density electrodeposition of nickel foam

Plating region	1	2	3	4	5
a_i	1.00	1.72	3.04	3.71	5.04
L_i/m	0.247	0.424	0.750	0.915	1.240
l_i/m	0.100	0.058	0.189	0.155	0.288

$D(0) = 0.1$ m; $D = 0.02$ m; $A = 0.5$ kg m^{-2}; $\rho_L = 0.214$ Ω m.

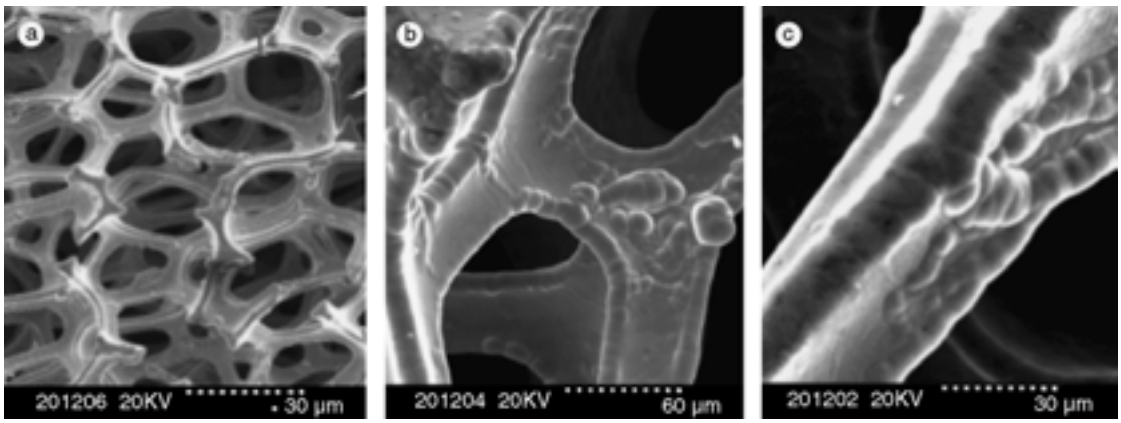

Fig. 3. Microstructure of the nickel foam produced under non-constant current density electrodeposition. (a) Net structure; (b) and (c) surface morphology of deposited nickel.

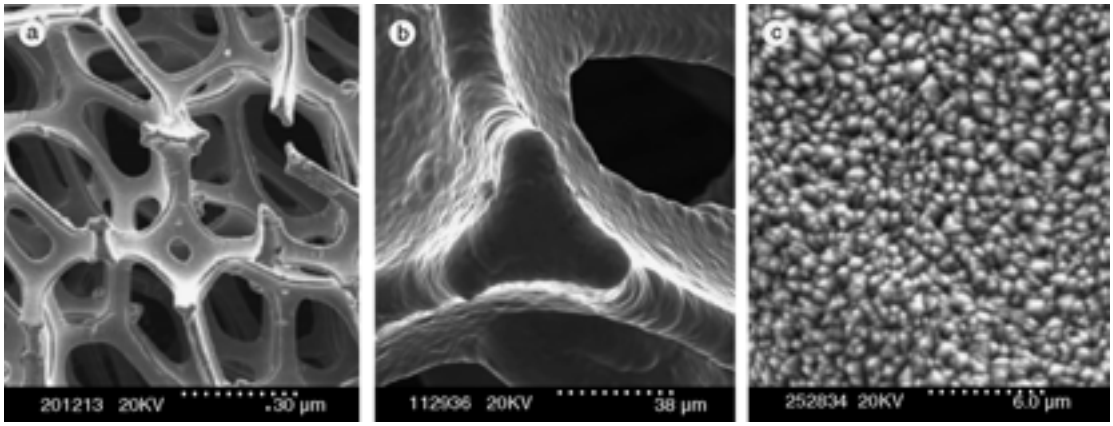

Fig. 4. Microstructure of the nickel foam produced under the five-step constant current density electrodeposition. (a) Net structure; (b) and (c) surface morphology of deposited nickel.

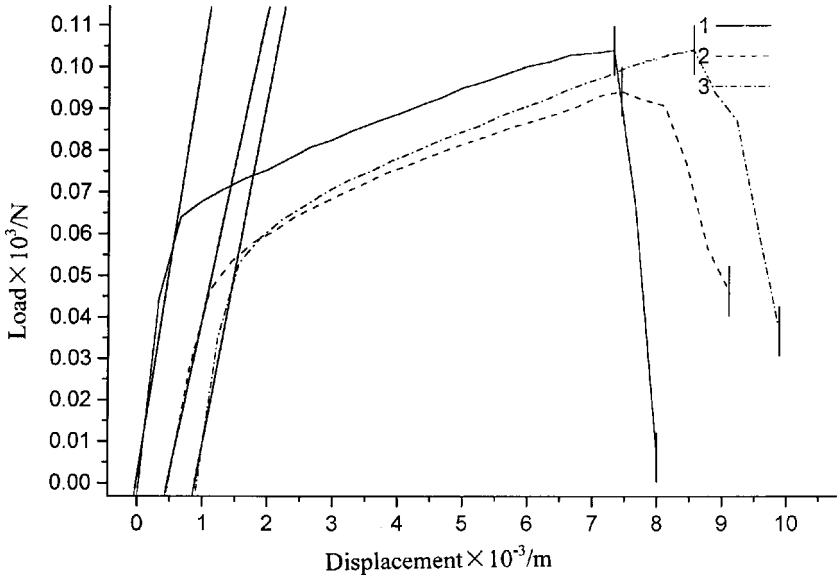

Fig. 5. Tensile curves of the nickel foam in longitudinal direction (three times repeat).

The mechanical characteristics of the nickel foam produced in the designed five-step constant current density electrodeposition were evaluated by measuring the longitudinal and latitudinal tensile strength σ_b and

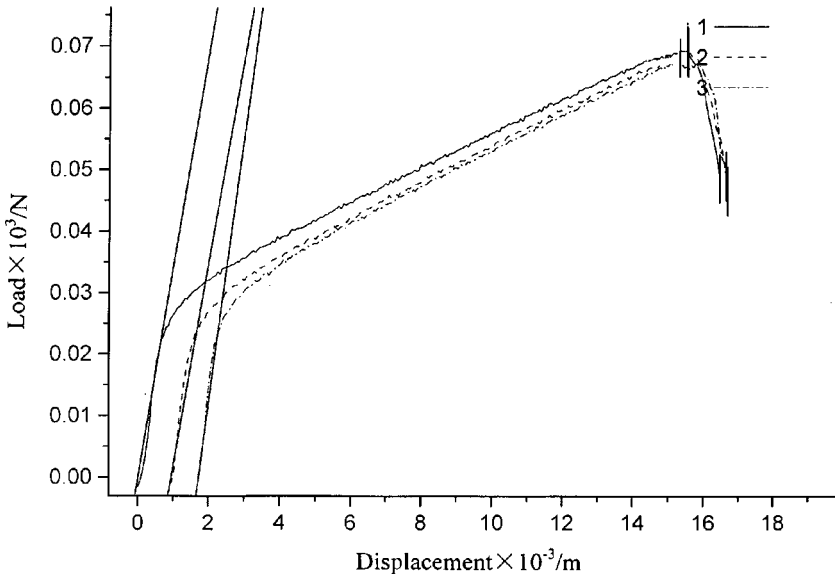

Fig. 6. Tensile curves of the nickel foam in latitudinal direction (three times repeat).

Table 3. Ultimate tensile strength and percent elongation of nickel foam produced in the five-step constant current density electrodeposition

	Longitudinal direction	Latitudinal direction
σ_b MPa	2.10	1.43
δ %	8.55	15.8

elongation δ. Each measurement was repeated three times. The tensile curves of the nickel foam in the longitudinal and latitudinal directions are shown in Figures 5 and 6, respectively. The average ultimate tensile strength σ_b and the percent elongation δ are listed in Table 3. Compared with the nickel foam produced under non-constant current density electrodeposition reported previously [13, 14], the mechanical characteristics of the nickel foam produced in the five-step constant current density electrodeposition were improved significantly.

6. Conclusion

A mathematical model is established to analyse multi-step constant current density electrodeposition for continuous porous metal production. The relationship between the anode length in each step, layout of the anode, and velocity of the cathode movement are investigated. The optimum cathodic current density is determined. The predicted parameters were successfully used to design the multiple-step constant current density electrodeposition of continuous nickel foam. The properties of continuous nickel foam thus produced were improved.

References

1. J. Babjak, V.A. Ettle and V. Paserin, *EP 0 402 738 A2* (1990).
2. J.R. Brannan, A.S. Bean and A.J. Vaccaro, *US Patent 5 098 544* (1992).
3. M.L. Soria, J. Chacón and J.C. Hemández, *J. Power Sources* **102** (2001) 97.
4. P.S. Liu, B. Yu and M.A. Hu, *Trans. Nonferrous Metals Soc., China* **11** (2001) 629.
5. P. Cognet, J. Berlan and G. Lacoste, *J. Appl. Electrochem.* **26** (1996) 631.
6. L. Bonnefoi, P. Simon and J.F. Fauvarque, *J. Power Sources* **83** (1999) 162.
7. S. Langlois and F. Coeuret, *J. Appl. Electrochem.* **19** (1989) 43.
8. P.S. Liu, M. Lu, T.F. Li and C. Fu, *Mater. Sci. Technol.* **7** (1999) 77.
9. P.S. Liu, T.F. Li, C. Fu and M. Lu, *Rare Metal Mater. & Eng.* **28** (1999) 260.
10. P.S. Liu, C. Fu and T.F. Li, *Science in China* (Series E) **28** (1999) 193.
11. S. Langlois and F. Coeuret, *J. Appl. Electrochem.* **19** (1989) 51.
12. T. Doherty, J.G. Sunderland and E.P.L. Roberts, *Electrochim. Acta* **41** (1996) 519.
13. L. Xia, H. Wu and H.Q. Jia, China International Battery Fair 2001, Bejing (2001), p. 156.
14. C.S. Dai, D.L. Wang and X.G. Hu, Proceedings of the 24th China National Chemical and Physical Power Sources, Harbin (2000), p. 97.